STRUCTURAL CHEMISTRY

Volume 74 (2018)

Supporting information for article:

The effect of amino acid backbone length on molecular packing: crystalline tartrates of glycine, β-alanine, γ-aminobutyric acid (GABA) and dl-α-aminobutyric acid (AABA)

Evgeniy Losev and Elena Boldyreva

FTIR

Table S1-FTIR. Tentative assignment of vibrational modes for 5 mixed crystals of DL-tartaric acid with different amino acids

Assignment	Frequency (cm^{-1})				
	Gly-DL-tart (**I**)	β-ala-DL-tart, (**II**)	β-ala-DL-tart (**III**)	GABA-DL-tart (**IV**)	DL-AABA-DL-tart (**V**)
OH stretch / NH stretch / CH stretch[1]	3400	3447	3373	3418	3431
	3250	3316	3283	3391	3299
	3159	3268	3215	3290	3111
	3125	3150	3074	3247	3041
	3049	3056	3022	3160	2983
	2989	2992	2982	3115	2950
	2940	2963	2930	3064	2890
	2415	2949	2888	2983	2840
		2924	2671	2960	2776
		2835	2481	2947	2632
		2768		2922	2545
		2450		2902	
				2884	
				2835	
				2768	
				2676	
				2595	
				2499	
C=O stretch	1712	1714	1724	1738	1739
NH_3^+ as bend	1592	-	1604	1693	1623
			1586		1599
COO^- as stretch	1573	-	-	1650	-
				1622	
NH_3^+ sym bend	-	1519	1515	1526	1511
CH_2 scissor/ CH_3 as bend	1476	1474		1474	1472
		1458			1464
		1431			1444

		1410			1430
COO^- sym stretch	1423	-	-	1447	-
CH_2 wagg / CH_3 sym bend[2]	1310	1378	1391	1392	1364
		1333			1342
CH_2 twist	1272	1270	1295	1226	1248
	1227	1229	1266		
	1210	1201	1243		
CH_3 rock	-	-	-	-	1197
NH_3^+ rock	1119	1115	1121	1153	1118
	1091	1097	1102	1118	1085
	1080	1079	1073	1112	
		1048		1081	
CC stretch	910	928	939	964	930
	901				
CH_2 rock	755	755	753	760	791
	712				755

1 – N-H stretching vibrations show as wide band between 3450-2500 cm^{-1}. C-H stretching vibrations superimposed on N-H stretch

2 – for DL-AABA-DL-tart (**V**)

Other medium and weak bands between 1200 and 600 cm^{-1} correspond to bending out-of-plane (oop) vibrations and skeletal vibrations.

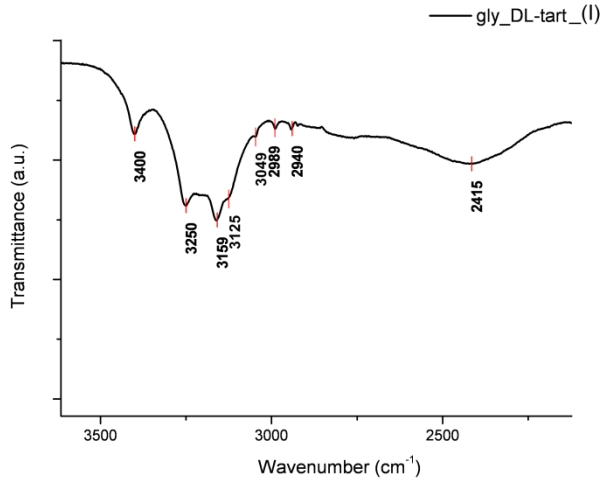

a

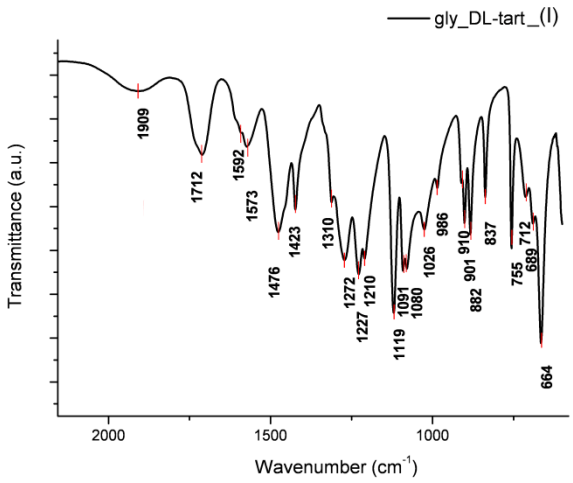

b

Figure S1-FTIR. FTIR ATR spectrum of glycine-DL-tartaric acid cocrystal (**I**)

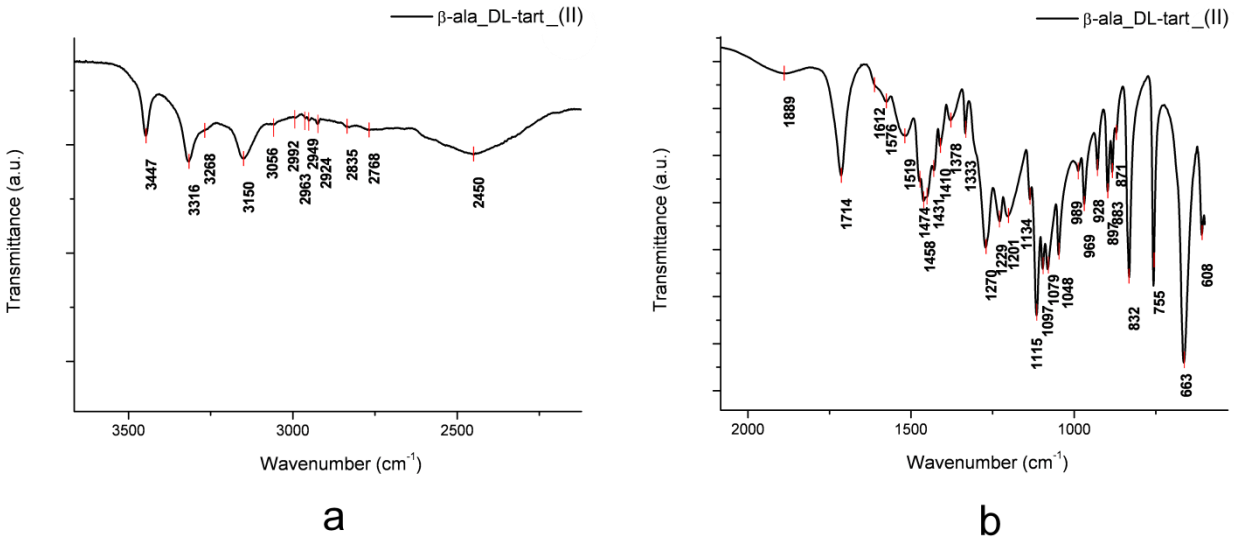

Figure S2-FTIR. FTIR ATR spectrum of β-alanine-DL-tartaric acid cocrystal (**II**)

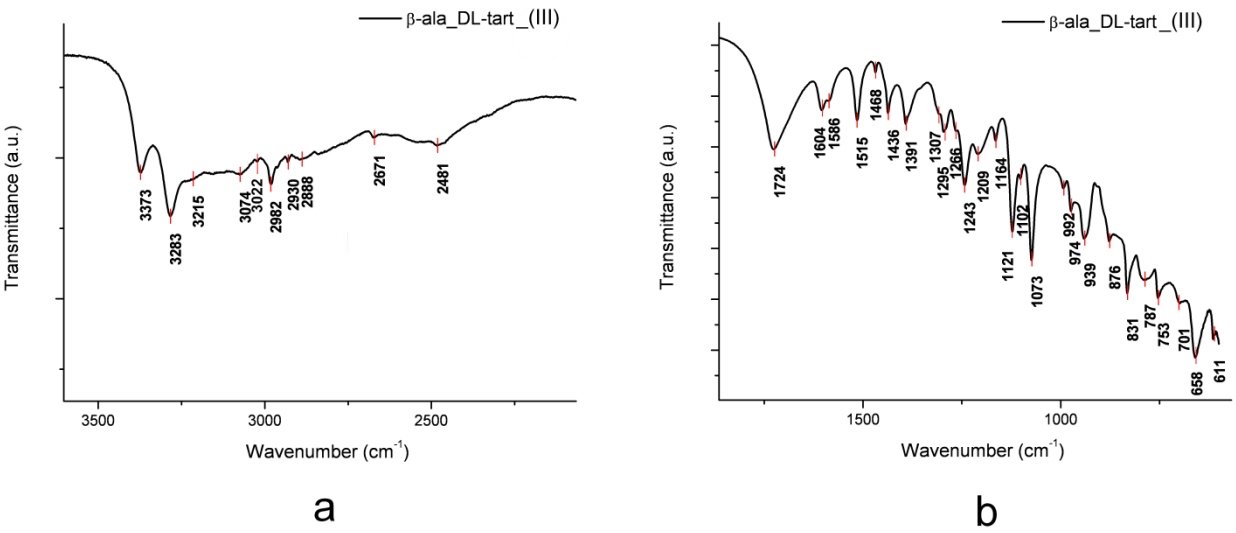

Figure S3-FTIR. FTIR ATR spectrum of β-alanine-DL- tartaric acid molecular salt (**III**)

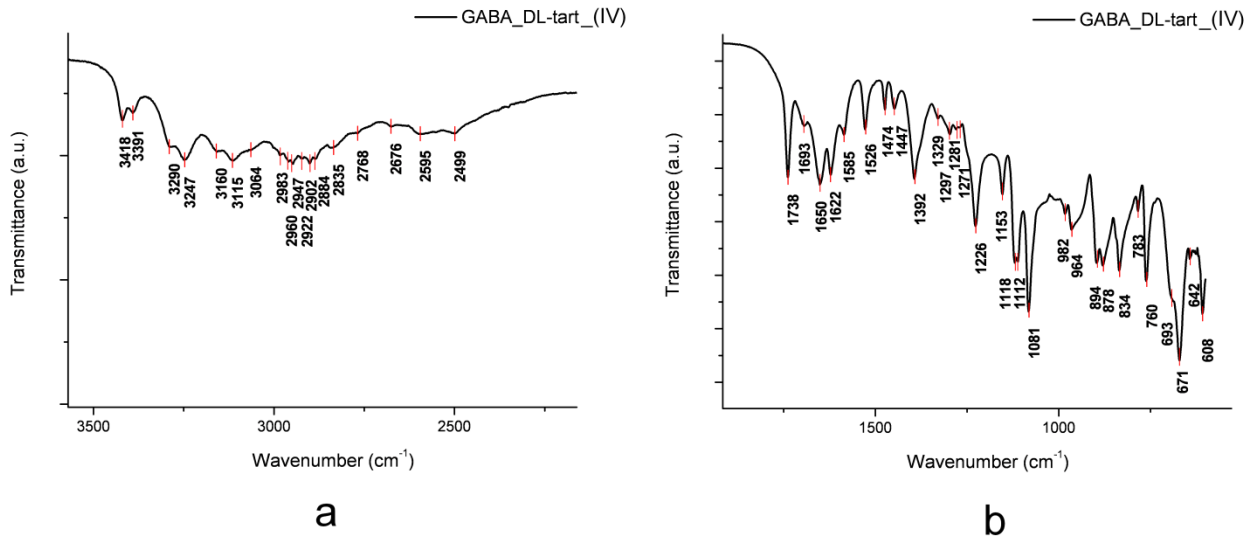

Figure S4-FTIR. FTIR ATR spectrum of GABA-DL- tartaric acid molecular salt (**IV**)

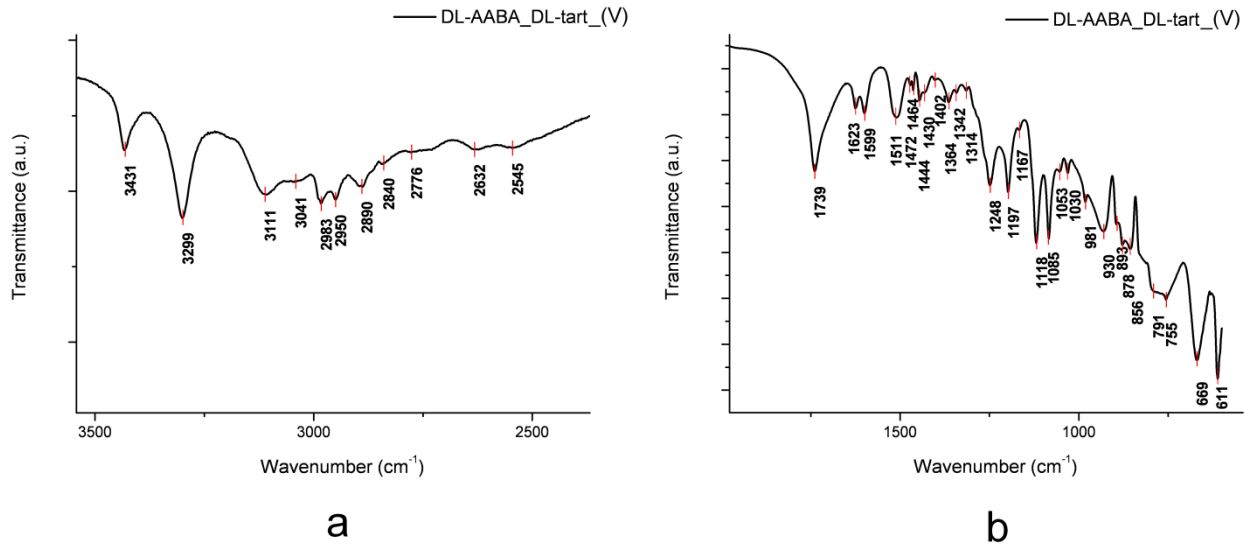

Figure S5-FTIR. FTIR ATR spectrum of DL-AABA-DL- tartaric acid molecular salt (**V**)

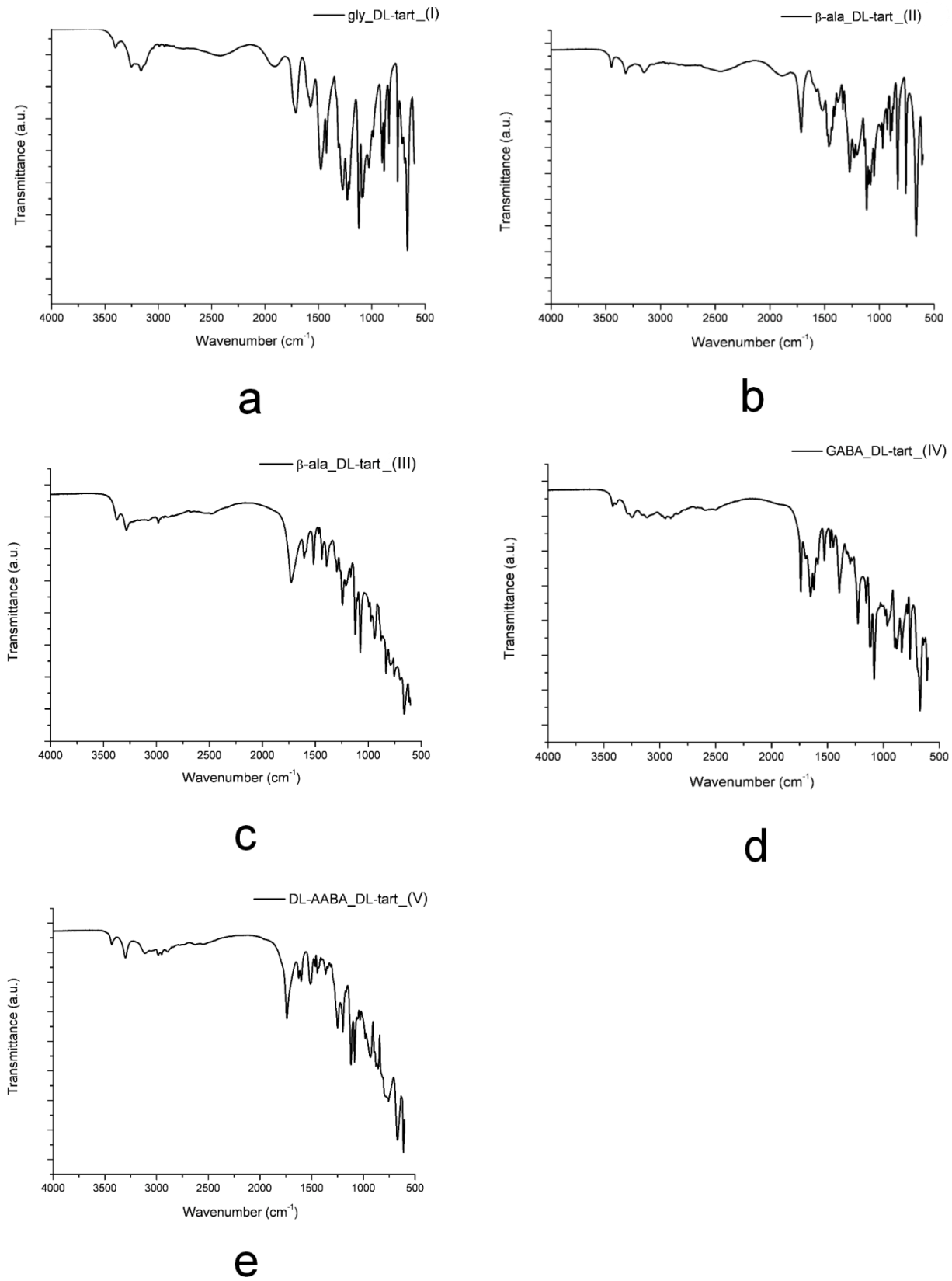

Figure S6-FTIR. FTIR ATR spectra of 5 mixed crystals of DL-tartaric acid. a -glycine-DL-tartaric acid (**I**); b – β-alanine-DL-tartaric acid (**II**); c - β-alanine-DL- tartaric acid (**III**); d – GABA-DL-tartaric acid (**IV**); e – DL-AABA-DL- tartaric acid (**V**)

Table S2-HB. Selected hydrogen-bond parameters for four novel crystal structures

D—H···*A*	*D*—H (Å)	H···*A* (Å)	*D*···*A* (Å)	*D*—H···*A* (°)
beta-ala_DL-tart_(II)				
O4—H4···O3^{i}	0.82	2.21	2.8778 (15)	139.0
O3—H3···O4^{ii}	0.82	1.99	2.8048 (15)	174.9
O6—H6···O8^{iii}	0.82	1.76	2.5728 (15)	172.8
O1—H1···O7^{iv}	0.82	1.74	2.5240 (16)	159.7
N1—H1A···O8^{v}	0.89	2.05	2.8477 (17)	149.3
N1—H1C···O7	0.89	2.22	2.8508 (17)	127.3
beta-ala_DL-tart_(III)				
O4—H4···O3^{ii}	0.82	1.97	2.7653 (17)	164.8
O1—H1···O7^{vi}	0.82	1.79	2.6092 (18)	174.0
N1—H1A···O4^{i}	0.89	2.56	3.142 (2)	123.8
N1—H1A···O5^{i}	0.89	2.16	3.017 (2)	160.6
N1—H1B···O5^{vii}	0.89	2.08	2.916 (2)	155.4
N1—H1B···O2^{viii}	0.89	2.52	3.064 (2)	120.5
N1—H1C···O2^{ix}	0.89	2.37	2.986 (2)	126.5
GABA_DL-tart_(IV)				
O27—H27···O18	0.82	1.76	2.5805 (19)	179.1
N21—H21A···O25^{x}	0.89	2.00	2.828 (2)	154.0
N21—H21B···O15^{xi}	0.89	2.11	2.8651 (19)	141.9
N21—H21C···O12^{xii}	0.89	2.13	2.966 (2)	155.1
O17—H17···O26	0.82	1.68	2.4663 (17)	160.9
N11—H11A···O25^{x}	0.89	2.01	2.8813 (19)	165.6
N11—H11B···O22^{xiii}	0.89	2.10	2.9105 (19)	150.5
N11—H11C···O15^{xi}	0.89	2.50	3.1013 (19)	125.5
N11—H11C···O16^{xiii}	0.89	2.12	2.8760 (19)	142.6
O21—H21···O16	0.82	1.66	2.4740 (16)	171.5
O23—H23···O13^{xiv}	0.82	2.06	2.7519 (17)	141.7
O24—H24···O14^{xv}	0.82	1.92	2.7346 (16)	174.1
O11—H11···O28^{xv}	0.82	1.82	2.6220 (19)	164.6
O13—H13···O23^{xvi}	0.82	1.91	2.7190 (15)	170.9
O14—H14···O24^{ii}	0.82	2.14	2.7986 (17)	137.8
DL-AABA_DL-tart_(V)				
O4—H4···O3^{ii}	0.82	1.94	2.7567 (13)	177.3
O3—H3···O4^{xi}	0.82	2.24	2.8961 (14)	137.5
O1—H1···O7	0.82	1.81	2.6228 (14)	169.2
N1—H1A···O4^{xvii}	0.89	2.30	2.8969 (16)	124.5
N1—H1A···O5^{xvii}	0.89	2.02	2.8785 (16)	160.6
N1—H1B···O5^{xviii}	0.89	2.15	2.9887 (19)	155.8

N1—H1C···O2^{xix}	0.89	2.08	2.8733 (16)	147.5
N1A—H1AA···O5^{xvii}	0.89	1.89	2.761 (16)	164.8
N1A—H1AB···O2^{xix}	0.89	2.14	2.970 (16)	154.0
N1A—H1AC···O7^{xix}	0.89	1.96	2.745 (17)	145.8
C7A—H7AA···O6^{xv}	0.97	2.28	3.03 (2)	133.2

Symmetry code(s): (i) -*x*+1, -*y*+1, -*z*; (ii) *x*+1, *y*, *z*; (iii) -*x*+2, *y*+1/2, -*z*+1/2; (iv) *x*-1, -*y*+3/2, *z*-1/2; (v) -*x*+1, *y*+1/2, -*z*+1/2; (vi) -*x*+2, -*y*+2, -*z*+1; (vii) -*x*, -*y*+1, -*z*; (viii) *x*-1, *y*-1, *z*; (ix) *x*, *y*-1, *z*; (x) -*x*, -*y*+1, -*z*+2; (xi) -*x*+1, -*y*+1, -*z*+2; (xii) *x*-1, *y*, *z*+1; (xiii) *x*, *y*+1, *z*+1; (xiv) *x*-1, *y*, *z*; (xv) -*x*+1, -*y*, -*z*+1; (xvi) -*x*+1, -*y*+1, -*z*+1; (xvii) *x*, *y*, *z*-1; (xviii) *x*+1, *y*, *z*-1; (xix) -*x*+2, -*y*+1, -*z*+1.

Hot Stage Microscopy

Hot stage microscopy observations for **I**, **II**, **III**, **IV**, **V**

Figure S1-HSM. Melting of the glycine-DL-tartaric acid cocrystal (**I**). Beginning of the process at 162°C observed as a slight deformation of the right side of the needle. The start of the process could be also seen by minor change of the polarization of the right tip of the needle. Then a slight shading of the whole crystal can be seen at 168°C, and the dark spots form between 174-178°C, giving evidence of the start of decomposition. The process is finished at 185°C. There were no changes in the crystal below 158°C.

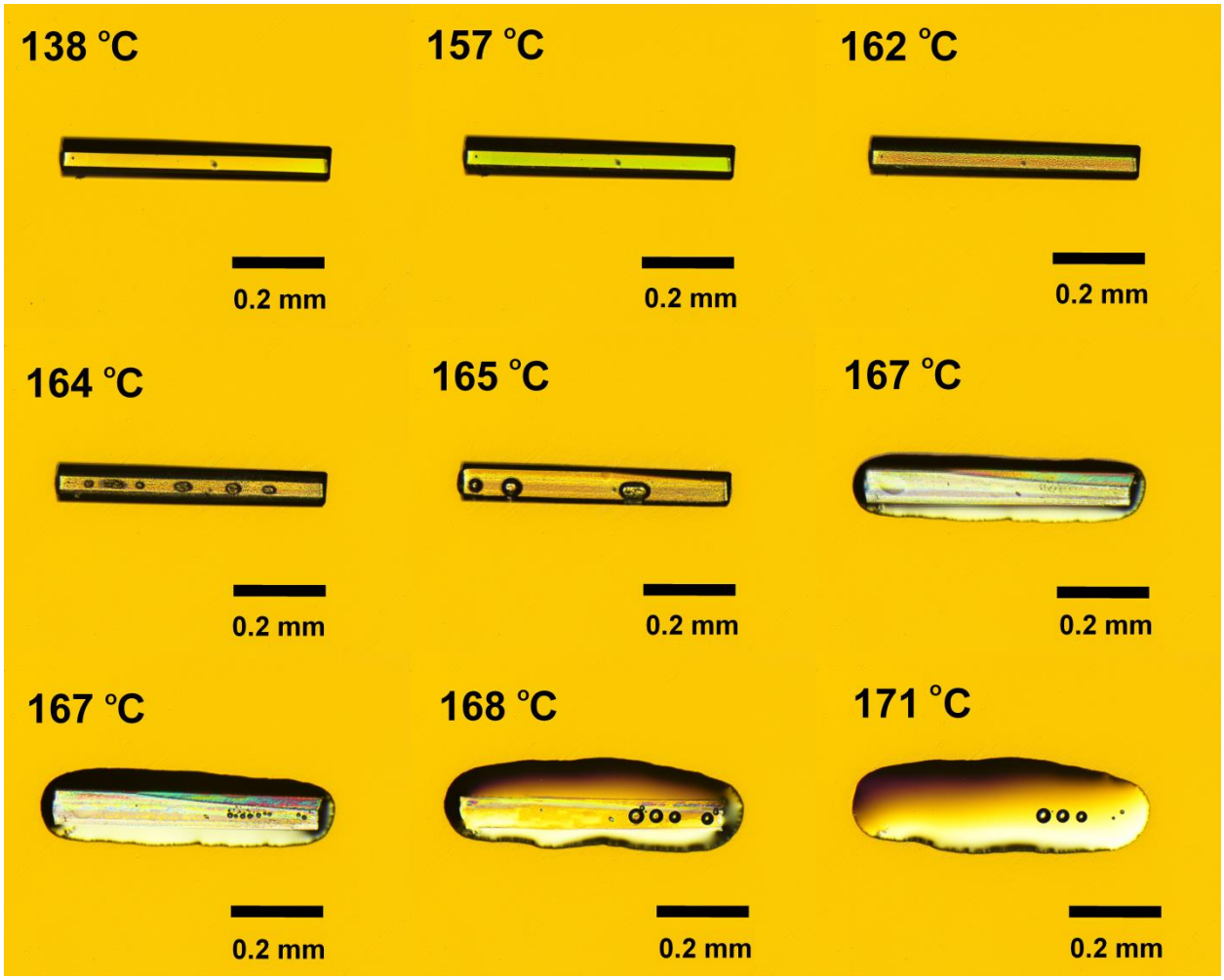

Figure S2-HSM. Melting accompanied by the decomposition of the β-alanine-DL-tartaric acid cocrystal (**II**). The process starts at 157°C when the color of the crystal as observed in polarized light changes. The crystal becomes pale at 162°C. The gas bubbles are formed between 164 and 171°C, this gives evidence that melting is accompanied by decomposition. No changes were observed below 138°C.

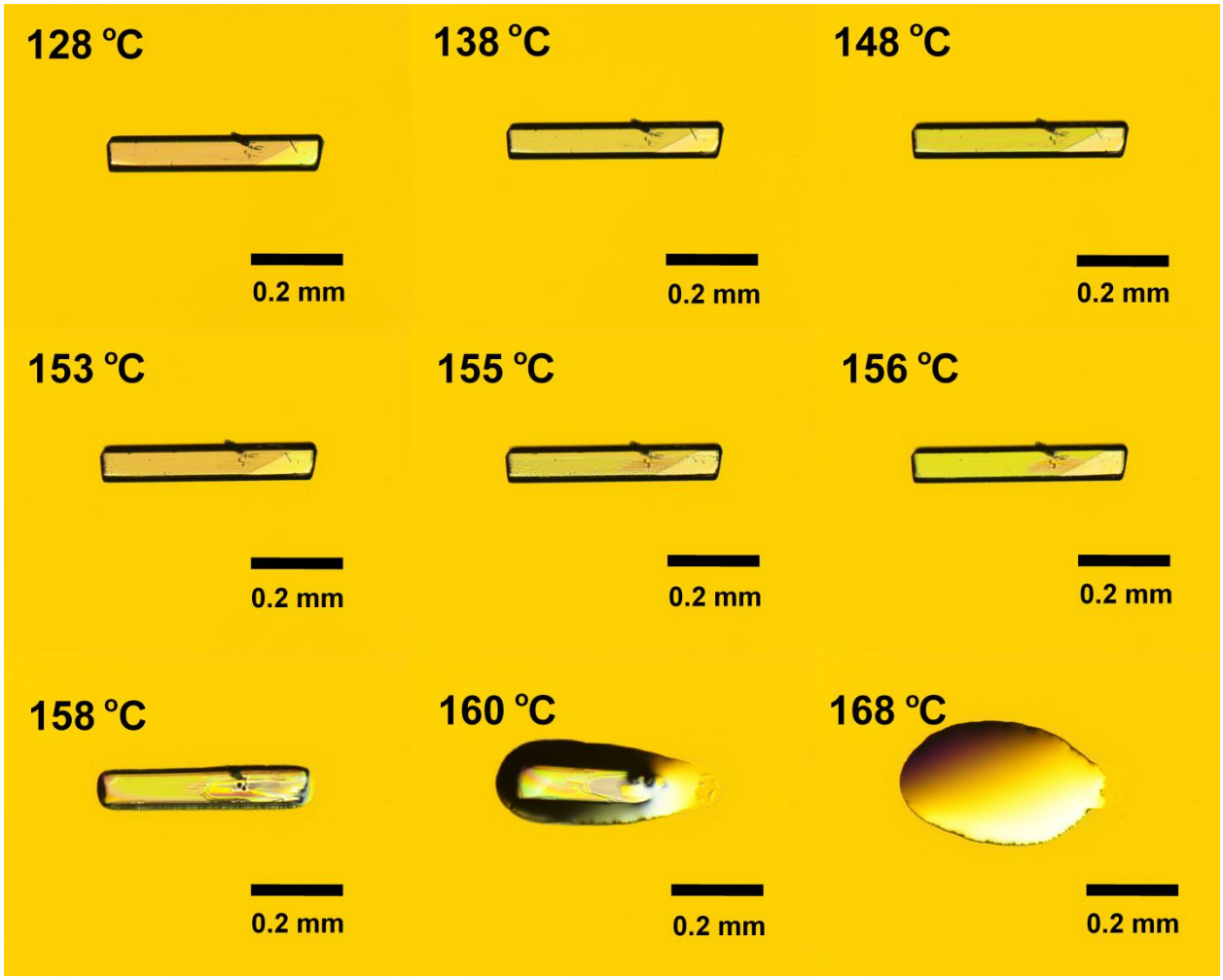

Figure S3-HSM. Melting of the β-alaninium tartrate (**III**). The color of the crystal observed in polarized light changed between 128 and 148°C. At 153°C the "color" of the crystal looked again as at 128°C. Some visual defects started to appear at 155°C. Complete melting could be observed at 168°C. There were no changes in the crystal below 128°C.

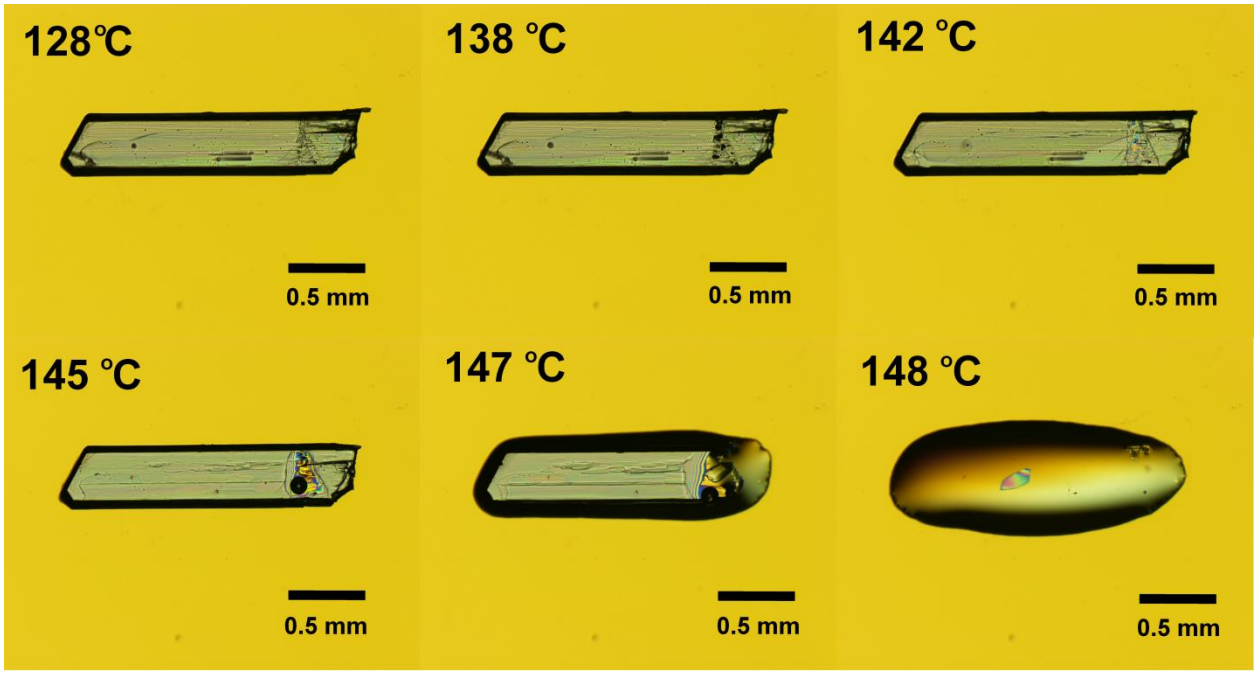

Figure S4-HSM. Melting of the GABA-DL-tartrate (**IV**). The black spots appear at 138°C. The melting of the top right corner of the crystal was observed at 142°C. The gas bubble formed at 145°C. Melting was complete at about 148°C. No changes in the crystal were observed below 128°C.

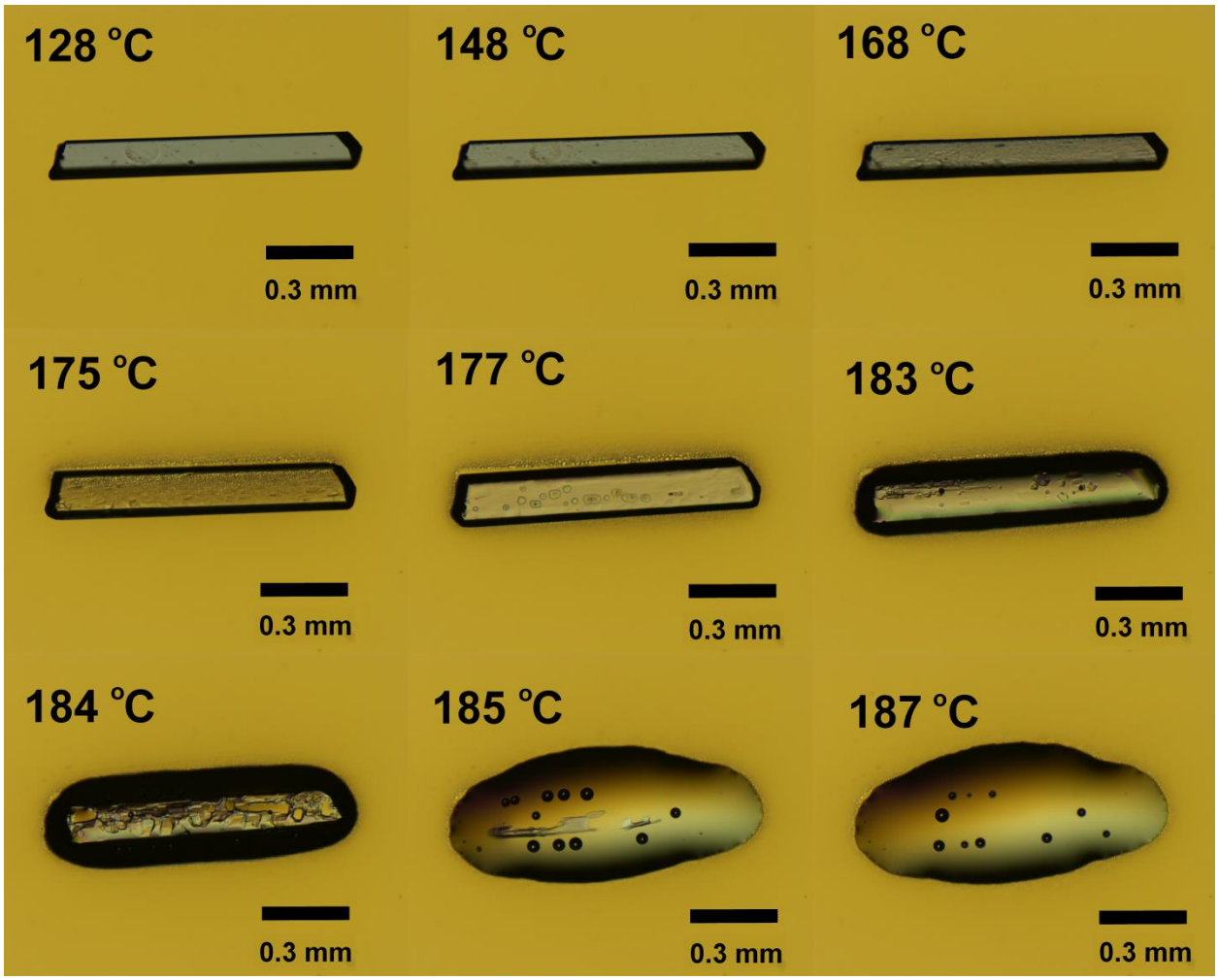

Figure S5-HSM. Melting of the DL-AABA- tartrate (**V**). Some defects appeared between 148°C and 168°C (assumed as the start of melting). The crystal suddenly moved between 168 and 175°C apparently due to the local melting at one of the crystal edges. The melting with the formation of gas bubbles was observed between 183°C and 187°C. There were no changes in the crystal below 128°C.

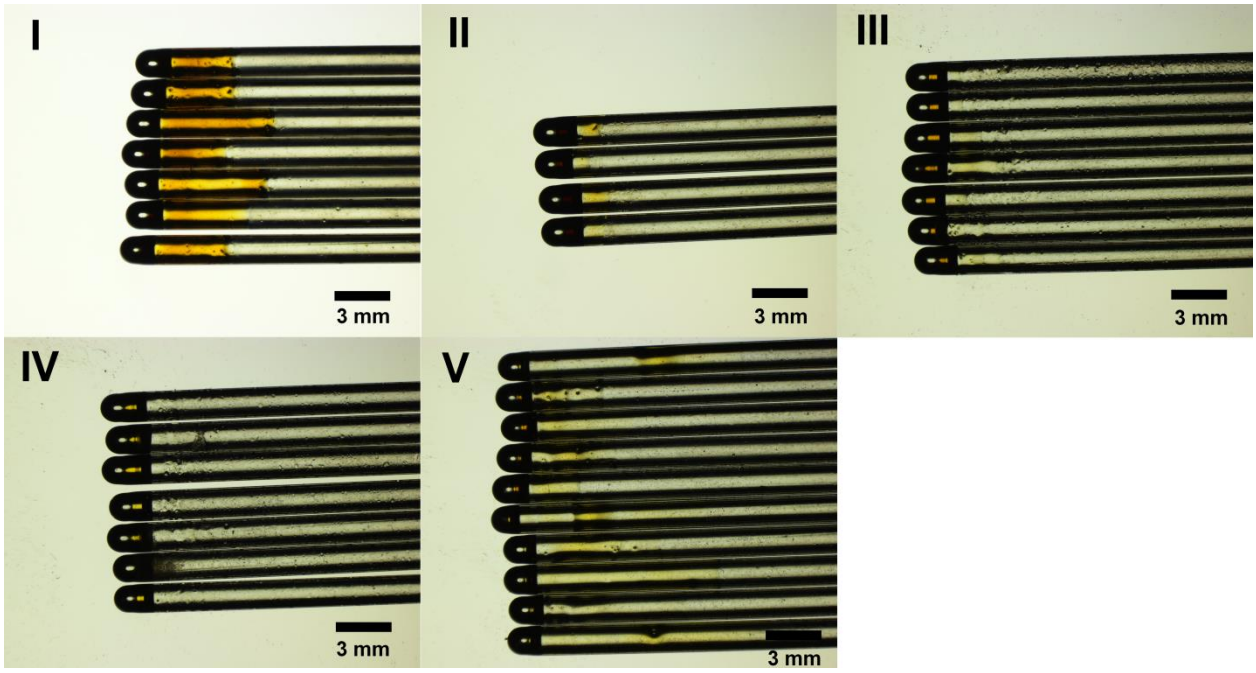

Figure S6-HSM. Glass capillaries after the experiments on determination of the melting point using BÜCHI M-560. The yellowing of the melt and of the walls of these capillaries evidence that melting was accompanied by decomposition.